

TWO DIMENSIONAL MULTI-PORT METHOD FOR ANALYSIS OF PROPAGATION CHARACTERISTICS OF SUBSTRATE INTEGRATED WAVEGUIDE

E. Abaei¹, E. Mehrshahi¹, G. Amendola², E. Arneri², and A. Shamsafar^{2,*}

¹Department of Electrical Engineering, Shahid Beheshti University, G. C., Tehran, Iran

²Dipartimento di Elettronica, Informatica e Sistemistica, Università della Calabria, 87036 Rende (CS), Italy

Abstract—In this paper, two dimensional multi-port method is used to analyze substrate integrated waveguide by using Green's function approach to obtain the impedance matrix of equivalent planar structure. Modes propagation constant of substrate integrated waveguide, as a periodic structure, is calculated by applying Floquet's theorem on the impedance matrix of a unit cell. Field distribution of the propagating mode is obtained by this method. Results obtained by this method are verified, in a broad range of dimensions, by comparing with published results and also those calculated by commercial electromagnetic simulator, HFSS. Electromagnetic band gaps and mode conversion phenomenon as properties of periodic structures are also observed and investigated. Mode conversion in SIW is reported for the first time by our proposed method.

1. INTRODUCTION

Substrate integrated waveguide (SIW) is a promising candidate for circuits and components operating in microwave, millimeter wave and terahertz regions. This waveguide-like structure preserves most the advantages of conventional rectangular waveguides, such as high quality-factor and high power-handling capability. SIW has been widely used in planar microwave circuits in recent years [1–5], and various numerical methods have been developed to analyze these structures [6–10].

Received 25 February 2012, Accepted 2 May 2012, Scheduled 30 May 2012

* Corresponding author: Alireza Shamsafar (ashamsafar@deis.unical.it).

Two dimensional multi-port method — or planar circuit approach — involves determination of impedance matrix (Z -matrix) of the planar structure by using Green's function. In this method, Green's functions are employed to obtain multi-port impedance matrix of the model by assuming several ports along the peripheries of the structure. This numerical method with some changes was employed for characterizing SIW, named H -plane planar circuit approach [9]. Since this method contains some vagueness of the excitation region, TRL calibration technique was applied to the calculation of propagation constant of SIW [10]; also the model contains more than one period. But since the SIW is a periodic structure, propagation characteristics can be obtained from one period model and without any excitation.

In this paper, two-dimensional (2-D) multi-port is used to analyze propagation characteristics of SIW, however with different procedures as in [10], to calculate the circuit Z -matrix and also propagation constant. In our work, the width of each port is taken to be much smaller than the wavelength to make sure that the field distribution is almost constant along the ports. Then, using Floquet's theorem for periodic structures, propagation constant of SIW modes is obtained from a unit cell Z -matrix (\mathbf{Z}_U). Field distribution of SIW modes is also obtained by this method. The results of the proposed method are valid in a broad range of dimensions [6].

Although the SIW structure has similar properties to conventional waveguides, obviously there are some differences. Electromagnetic band gaps (EBGs), as a property of periodic structures, is one of these differences, reported by some numerical methods, such as finite difference frequency domain (FDFD) [8]. Mode conversion is another property of periodic structures, which is analytically and experimentally investigated in photonic crystal channel waveguides (PCCW), a periodic waveguide with a similar structure to SIW [11]. However, for the first time mode conversion in SIW is reported by the proposed method [12]. As will be shown in numerical results, mode conversion also causes non-propagating bands. Mode conversion and differences between mode conversion with conventional EBG will be discussed.

This paper is organized as follows. In Section 2, 2-D method is used to model a unit-cell of periodic SIW. As explained in Section 3, applying Floquet's theorem leads to an eigenvalue problem that gives propagation characteristics of SIW modes. EBG and mode conversion phenomena in SIW, as properties of periodic structures, are discussed in Section 4. Results obtained by this method are compared with published results and also those obtained by electromagnetic full wave simulator, HFSS, in Section 5.

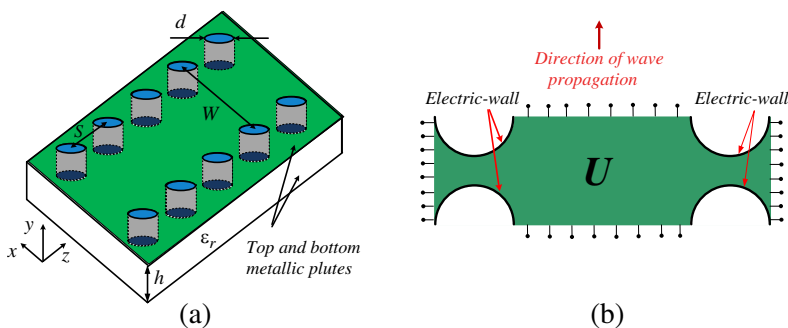


Figure 1. (a) Geometry of SIW structure. (b) Top view of a unit cell of SIW.

2. STRUCTURE AND METHOD OF ANALYSIS

Figure 1(a) shows a SIW structure composed of two parallel rows of conducting cylinders with period length “ s ” and diameter “ d ”, and two conductor surfaces which cover top and bottom of the substrate. In this structure, the height is much less than the wavelength so that electromagnetic field is constant in the height of substrate. Moreover, it is periodic, so propagation characteristics of SIW are obtained from planar model of a unit cell, shown in Figure 1(b).

As can be seen in Figure 1(b), there are several ports along periphery of the circuit. In 2-D method, the planar circuit is modeled by the impedances between the ports [13]. Consider the arbitrary planar circuit shown in Figure 2. In 2-D method, electric field E_y is used to define a voltage “ V ” between the planar circuit conductor and the ground plane. This voltage is obtained as

$$V = -E_y h \tag{1}$$

where h represents the spacing between the two conductors. If the planar component is excited by a current density J_y in the y -direction at any arbitrary point (x_0, z_0) inside the periphery, the wave equation can be written as

$$\left(\frac{\partial}{\partial x^2} + \frac{\partial}{\partial z^2} + k^2 \right) V = -j\omega\mu h J_y \tag{2}$$

where k is the wave number of the spacing material. On the other hand, when the planar circuit is edge-fed, the term J_y denotes a fictitious current density injected normally into the circuit (\mathbf{n} in Figure 2 shows the unit vector normal to the circuit). In this case, the current density

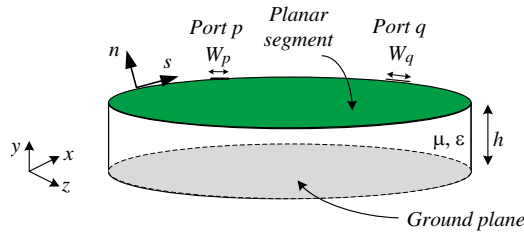


Figure 2. A planar circuit of arbitrary shape.

is as

$$J_n = \frac{1}{j\omega\mu h} \frac{\partial V}{\partial n} \quad (3)$$

and injected into the circuit at coupling ports located along the periphery can be equivalently considered as fed normal to the circuit (along the y -direction) with magnetic wall boundary condition being imposed all along the periphery. The equivalent fictitious surface current J_s (in the y -direction) is obtained as

$$J_s = \frac{1}{j\omega\mu h} \frac{\partial V}{\partial n} \vec{a}_y \text{ (A/m)}. \quad (4)$$

Thus for edge-fed excitation, we can consider the planar circuit as being excited by y -directed line currents located at the coupling ports [13].

The solution for the wave equation given by (2) can be obtained using Green's function approach. The Green's function $G(r|r_0)$ for (2) is obtained by applying a unit line current source $\delta(r - r_0)$ flowing along the y -direction and located at $r = r_0$, which is a solution of

$$\left(\frac{\partial}{\partial x^2} + \frac{\partial}{\partial z^2} + k^2 \right) G(r|r_0) = -j\omega\mu h \delta(r - r_0) \quad (5)$$

With magnetic wall boundary condition. Since the source current is present only at the coupling ports, the voltage V at the periphery can be written as

$$V(s) = \sum_{W_q} \int G(s|s_0) J_s(s_0) ds_0 \quad (6)$$

where the summation is over all coupling ports; W_q indicates the width of q th coupling port; s and s_0 are the distances measured along the periphery. From Equations (3) and (4), we see that the current I_q fed at the q th coupling port can be written in terms of the y -directed

equivalent line current as

$$I_q = \int_{W_q} J_s(s_0) ds_0 \tag{7}$$

If the widths of the coupling ports are assumed to be small so that the line current density, J_s , is distributed uniformly over the port width, we have

$$I_q = W_q J_s(s_0) |_{\text{for the } q\text{th port}} \tag{8}$$

The voltage at p th port, v_p , is an average of voltage over the width of the port p . Substituting (8) into (6) gives the elements of the impedance matrix of the planar circuit as

$$z_{pq} = \frac{v_p}{I_q} = \frac{1}{W_q W_p} \int_{W_q} \int_{W_p} G(s|s_0) ds_0 ds, \tag{9}$$

So, for a given planar circuit, Z -matrix is obtained from the Green’s function. Although Green’s functions are only available for some regular shapes, segmentation and desegmentation methods can be used for irregular shapes [14, 15].

2.1. Z-matrix of a Unit Cell

As shown in Figure 1(b), the unit-cell can be assumed as a rectangle with four half-circles removed and electric wall on the curved boundaries. Z -matrices of both rectangular and half-circle segments are available [13], so desegmentation method [14], in four steps, is used to calculate Z_σ , as shown in Figure 3. Applying electric-wall boundary condition on the curved boundaries of σ -segment gives Z_U [6].

The unit-cell model shown in Figure 1(b) has ports at the lateral edges on the right and left sides, but in low leakage condition, propagation constant is not sensitive to termination impedance at these ports. So, it can be assumed that the ports located at these edges are open circuit (magnetic wall boundary condition). Hence, Z_U reduces to impedance parameters between the ports shown in Figure 4.

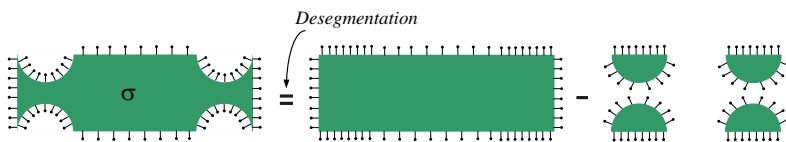


Figure 3. Desegmentation process for calculation of Z_σ .

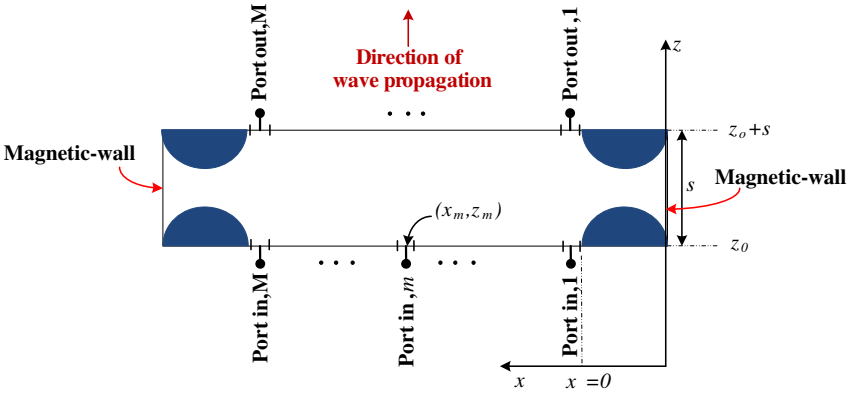


Figure 4. Ports locations in a unit cell of the periodic SIW.

3. PROPAGATION CHARACTERISTICS OF SIW MODES

Propagation characteristics of SIW as periodic structure are obtained by applying Floquet’s theorem on a unit-cell model shown in Figure 4. For this purpose, the unit-cell ports are defined as input ports and output ports located at $z = z_0$ and $z = z_0 + s$, respectively. By this definition, the Z -matrix of Figure 4 is divided to four sub-matrices as

$$\begin{bmatrix} v_{in,1} \\ \vdots \\ v_{in,M} \\ v_{out,1} \\ \vdots \\ v_{out,M} \end{bmatrix} = \begin{bmatrix} \bar{\bar{Z}}_{in,in}(1,1) & \dots & \bar{\bar{Z}}_{in,in}(1,M) & \bar{\bar{Z}}_{in,out}(1,1) & \dots \\ \vdots & \ddots & \vdots & \vdots & \ddots \\ \bar{\bar{Z}}_{in,in}(M,1) & \dots & \bar{\bar{Z}}_{in,in}(M,M) & \bar{\bar{Z}}_{in,out}(M,1) & \dots \\ \hline \bar{\bar{Z}}_{out,in}(1,1) & \dots & \bar{\bar{Z}}_{out,in}(1,M) & \bar{\bar{Z}}_{out,out}(1,1) & \dots \\ \vdots & \ddots & \vdots & \vdots & \ddots \\ \bar{\bar{Z}}_{out,in}(M,1) & \dots & \bar{\bar{Z}}_{out,in}(M,M) & \bar{\bar{Z}}_{out,out}(M,1) & \dots \end{bmatrix} \begin{bmatrix} I_{in,1} \\ \vdots \\ I_{in,M} \\ I_{out,1} \\ \vdots \\ I_{out,M} \end{bmatrix} \tag{10}$$

where $v_{in,m}$ and $I_{in,m}$ are voltage and current of m th input-port, and $v_{out,m}$ and $I_{out,m}$ are similarly defined. If the port width is assumed to be small enough compared with wavelength, then the voltage at each

port located at $z = z_0$ can be written as

$$v_{in,m} \cong V(x_m, z_0) = -hE_y(x_m, z_0) \tag{11}$$

where $E_y(x_m, z_m)$ is the electric field, at point $(x_m, y_m = h, z_m)$ in y -direction, so we have

$$\bar{v}_{in} = \begin{bmatrix} v_{in,1} \\ \vdots \\ v_{in,M} \end{bmatrix} \cong -h \begin{bmatrix} E_y(x_1, z_0) \\ \vdots \\ E_y(x_M, z_0) \end{bmatrix} \tag{12}$$

In the same way, by replacing z_0 with $(z_0 + s)$ in (12), \bar{v}_{out} is defined. If widths of all ports are equal, current vector \bar{I}_{in} will be written as

$$\bar{I}_{in} = \begin{bmatrix} I_{in,1} \\ \vdots \\ I_{in,M} \end{bmatrix} \cong \left(\frac{W - d}{M} \right) \begin{bmatrix} H_x(x_1, z_0) \\ \vdots \\ H_x(x_M, z_0) \end{bmatrix} \tag{13}$$

where “ $(W - d)/M$ ” is the width of each port. Employing Floquet’s theorem [16] leads to the following system

$$\begin{cases} \bar{v}_{out} = e^{-\gamma s} \bar{v}_{in} \\ \bar{I}_{out} = -e^{-\gamma s} \bar{v}_{in} \end{cases} \tag{14}$$

where, γ is the characteristic propagation constant. Circuit shown in Figure 4 is symmetric and reciprocal. Substituting (14) into (10) yields the following matrix eigenvalue system

$$\left(\bar{Z}_{in,out}^{-1} \bar{Z}_{in,in} - \cosh(\gamma s) \bar{U} \right) \bar{I}_{in} = 0 \tag{15}$$

where \bar{U} is an $M \times M$ identity matrix. The system in (15) has M eigenvalues $(\cosh(\gamma_m s); m = 1, 2, \dots, M)$. For real eigenvalues, if $\cosh(\gamma_m s) < 1$ then $\gamma_m = j\beta_m$, in which β_m is the phase constant of the propagating periodic wave and its related eigenvector, \bar{I}_{in} , which leads to field distribution of corresponding propagating wave, at the ports.

Since the propagating modes are TE_{n0} , the non-zero field components are H_x, H_z and E_y . Substitution of \bar{I}_{in} to (13) gives H_x (at the ports shown in Figure 4). E_y is calculated from (10) and (12). And H_z can be obtained using Maxwell equations as $H_z(x) = -j\omega\mu (\partial E_y \setminus \partial x)$.

According to (9), in lossless structure, all the Z_{ij} are pure imaginary. So $(\bar{Z}_{in,out}^{-1} \bar{Z}_{in,in})$ is a real matrix. For this reason, the eigenvalues must be real or conjugate pairs. For example, for the modes under the cutoff frequency, $\cosh(\gamma_m s)$ is real and bigger than one ($\gamma_m = \alpha_m$, where α_m is real and positive). However, the SIW analysis

shows that we cannot consider it as a propagating mode neither under cutoff frequency, in some narrow frequency bands. When $\cosh(\gamma_m s)$ becomes real and negative, or when eigenvalues are conjugate pairs, these phenomena happen. In the first case, $\gamma_m = \alpha_m + j(2k + 1)\pi/s$ ($k = 1, 2, \dots$) is related to EBGs of periodic structure of SIW. In the second case, $\gamma_m = \alpha_m + j\beta_m$ and $\gamma_n = \alpha_m + j(2k\pi - \beta_m)/s$. In this case, there is a non-propagating region for both “ m ” and “ n ” modes, which will be shown in the numerical results. This gap, also observed in PCCWs, is reported as characteristics of the SIW in this paper for the first time. In Section 4, the band gaps of the SIW will be discussed.

4. EBG AND MODE CONVERSION IN PERIODIC SIW

All periodic structures are subject to electromagnetic band gaps, in which small reflection from discontinuities interfere constructively, and the wave does not propagate. In periodic structure with period s , band gaps of the i th mode appear with following condition:

$$\beta_i \times s = k\pi; \quad k = 1, 2, 3, \dots \tag{16}$$

where β_i is propagation constant of the i th mode. Another property of periodic structures is mode conversion. In periodic structures, if

$$(\beta_i + \beta_j) \times s = 2k\pi; \quad k = 1, 2, \dots \tag{17}$$

then the i th mode will be coupled to the opposite propagating j th mode leading to energy transfer from i th to the j th mode, i.e., mode conversion [17].

As the simple periodic structures shown in Figure 5, it is obvious that all modes propagate without cross-coupling in the first structure, because there is not any discontinuity in all dimensions. But in the second one, modes with different longitudinal wave vectors will be coupled in dimensional discontinuities; this causes mode conversion at specified frequency presented in (17). In other words, EBGs happen in both structures, but mode conversion affects propagation characteristics only for the structure that shown in Figure 5(b) because of dimensional discontinuities in this structure [12].

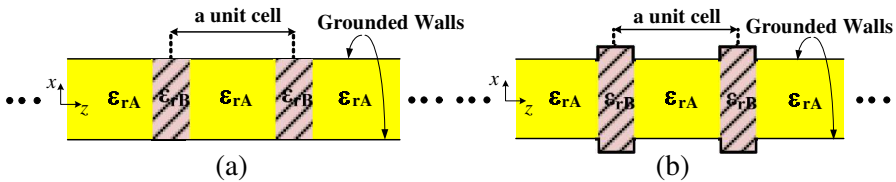


Figure 5. Two simple period structures, structure without dimensional discontinuities (a) structure with dimensional discontinuities (b).

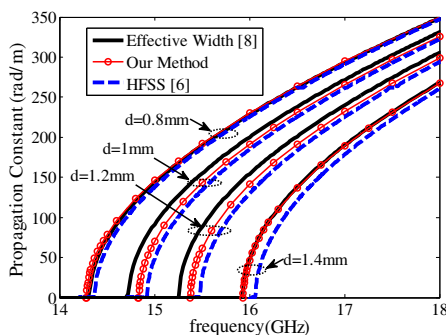


Figure 6. Propagation phase constant of SIW.

SIW is a periodic structure with dimensional discontinuities, so both EBG and mode conversion phenomena affect propagation characteristics.

5. NUMERICAL RESULTS

5.1. Propagation Characteristics of Fundamental Mode

In Figure 6, we compare propagation constants calculated by our method with equivalent rectangular waveguide [8], for different values of d . The dimensions are considered as: $s = 2\text{ mm}$, $W = 7.2\text{ mm}$, $h = 0.508\text{ mm}$ and $\epsilon_r = 2.33$. The results, obtained by HFSS simulator, are also depicted for comparison. All results are in good agreement as shown in Figure 6.

Figure 7 shows transverse variation of $H_x(x, z_0)$ and $E_y(x, z_0)$ for the fundamental mode, when $d = 1.4\text{ mm}$, at 17 GHz. As seen, $E_y(x)$ satisfies boundary conditions at $x = 0$ and $x = 5.8\text{ mm}$, and also it is symmetric around $x = 2.9$. According to Figure 7, characteristic impedance is $Z_c = 708.1717\ \Omega$, ($Z_c = -E_y/H_x$) which agrees with that obtained by effective width, $Z_c = 707.2\ \Omega$.

5.2. Mode Conversion in SIW

As we have mentioned earlier, periodic dimensional discontinuities of SIW affect propagation characteristics. Figure 8 shows phase constant of the SIW fundamental mode over a wide frequency band. The dimensions of the SIW are considered as: $d = 0.8\text{ mm}$, $s = 2.8\text{ mm}$, $W = 7.6\text{ mm}$, $h = 0.508\text{ mm}$ and $\epsilon_r = 2.33$. Phase constant of a rectangular waveguide with the same cut-off frequency, filled with $\epsilon_r = 2.33$, is also depicted. As shown in Figure 8, propagation constant

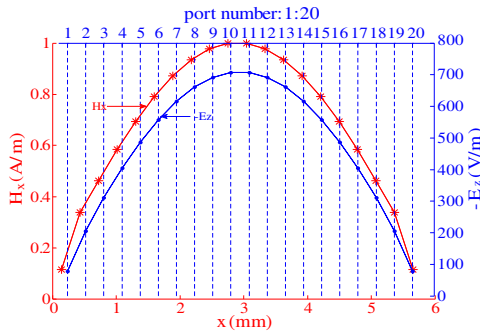


Figure 7. Variation of $H_x(x, z_0)$ and $E_y(x, z_0)$ for the fundamental mode (at the ports shown in Figure 4); $f = 17$ GHz, $M = 20$.

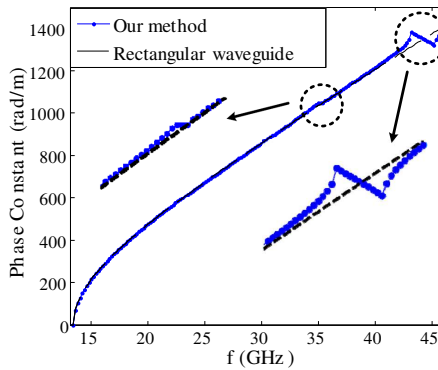


Figure 8. Phase constant of the SIW fundamental mode deviates from that of the equivalent rectangular waveguide at high frequencies.

of the SIW deviates from that of the rectangular waveguide at two frequency bands. Attenuation constant also peaks in these bands shown in Figure 9(a). The first stop band, also depicted by FDFD [8], is an electromagnetic band gap. In the band gap, attenuation constant reaches a maximum value of 20.1 m^{-1} , at 35.2 GHz, which agrees with those obtained by FDFD [8, Figure 19].

Since SIW is symmetric in x axis, fundamental mode couples with only odd modes. Figure 9(b) shows complex propagation constant of the third mode. As shown in Figures 9(a) and 9(b), propagation characteristics of both first and third modes deviate from their usual route at 43.2 GHz to 45.2 GHz, in which they have exactly the same attenuation constant. Phase delay per unit-cell of fundamental mode φ_1 ($\varphi_1 = \beta_1 \times s$), third mode φ_3 , and $\varphi_1 + \varphi_3$ are depicted in Figure 10.

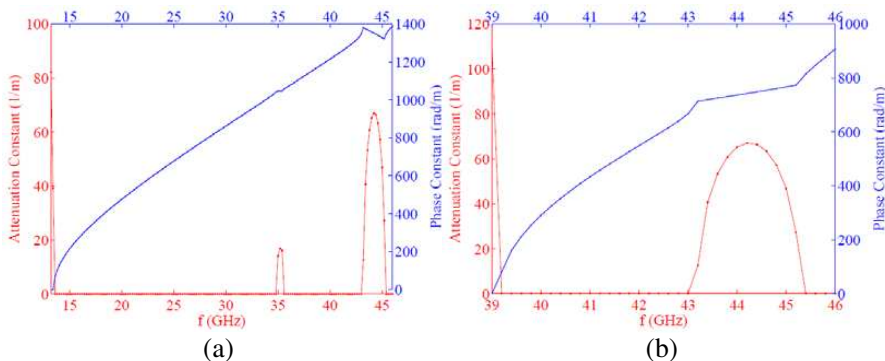


Figure 9. Complex propagation constant of SIW modes; fundamental mode (a) third mode (b).

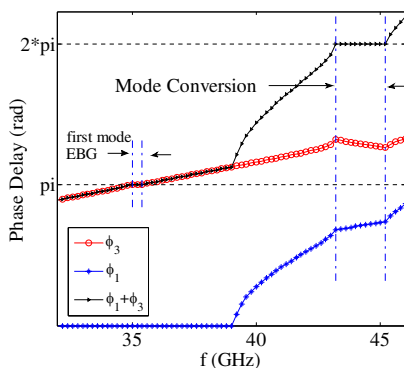


Figure 10. EBG and Mode conversion in SIW.

The results shown in Figure 10 confirm that EBG and mode conversion happen in 35 GHz to 35.4 GHz and 43.2 GHz to 45.2 GHz frequency bands, respectively. In the first frequency band, where $\varphi_1 = \pi$, wave does not propagate because small reflections from discontinuities interfere constructively, so that $\alpha \neq 0$ in this frequency band. In this band, there is not any interfering of high order modes. However, in the second gap, where $\varphi_1 + \varphi_3 = 2\pi$, the first and third modes affect each other. In this frequency band, the energy of the fundamental mode propagating in z -direction is transferred to the third mode in the opposite direction. Thus, the first mode cannot propagate in this frequency band. In the same way, energy of the third mode propagating in z -direction is transferred to the first mode. So, attenuation constant of both 1th and 3th modes peak when $\varphi_1 + \varphi_3 = 2\pi$. Mode conversion

in PCCWs is observed, in the same way, by a dip in the experimentally transmission spectra of the fundamental mode where the energy is transferred to the high order mode which propagates backward [11]. As shown in Figures 8–10, fundamental mode characteristics of SIW deviate from the rectangular waveguide, at high frequencies, due to weak dimensional discontinuities in this periodic structure.

6. CONCLUSION

This work presents an approach for the analysis of SIW, based on two-dimensional multi-port method. Propagation constant of SIW modes is obtained by applying Floquet's theorem on the impedance matrix of the unit cell. The results for fundamental mode are in good agreement with that in [8] and also verified by HFSS.

EBG and mode conversion phenomena as the properties of periodic structures with dimensional discontinuities are investigated by employing two simple periodic structures and their differences are discussed. The numerical results, compatible with other published results, show conventional EBGs. Additionally, mode conversion is also observed. Mode conversion in SIW is reported for the first time, by our proposed method.

REFERENCES

1. Kim, K., J. Byun, and H.-Y. Lee, "Substrate integrated waveguide Wilkinson power divider with improved isolation performance," *Progress In Electromagnetics Research Letters*, Vol. 19, 41–48, 2010.
2. Wang, Z., et al., "Half mode substrate integrated folded waveguide (HMSIFW) and partial H -plane bandpass filter," *Progress In Electromagnetics Research*, Vol. 101, 203–216, 2010.
3. Lin, S., S. Yang, A. E. Fathy, and A. Elsherbini, "Development of a novel UWB vivaldi antenna array using SIW technology," *Progress In Electromagnetics Research*, Vol. 90, 369–384, 2009.
4. Liu, C. J. and K. Huang, "A compact substrate integrated waveguide band-pass filter," *PIERS Proceedings*, 1135–1138, Cambridge, USA, July 5–8, 2010.
5. Wang, R., L.-S. Wu, and X.-L. Zhou, "Compact folded substrate integrated waveguide cavities and bandpass filter," *Progress In Electromagnetics Research*, Vol. 84, 135–147, 2008.
6. Abaei, E., E. Mehrshai, and H. R. Sadreazami, "Analysis of substrate integrated waveguide based on two dimensional

- multi-port method,” *International Conference on Microwave and Millimeter wave Technology (ICMMT)*, 793–796, 2010.
7. Arnieri, E. and G. Amendola, “Analysis of substrate integrated waveguide structures based on the parallel-plate waveguide Green’s function,” *IEEE Trans. on Microw. Theory and Tech.*, Vol. 56, No. 7, 1615–1623, 2008.
 8. Feng, X. and K. Wu, “Guided-wave and leakage characteristics of substrate integrated waveguide,” *IEEE Trans. on Microw. Theory and Tech.*, Vol. 53, No. 1, 66–73, 2005.
 9. Kishihara, M., K. Yamane, and I. Ohta, “Analysis of post-wall waveguide by H -plane planar circuit approach,” *IEEE/MTT-S International Microwave Symposium*, 1931–1934, 2007.
 10. Zhubenko, V., “Passive microwave components and antennas,” In-Tech, 2010.
 11. Olivier, S., et al., “Coupled-mode theory and propagation losses in photonic crystal waveguides,” *Opt. Express*, Vol. 11, No. 13, 1490–1496, Jun. 2003.
 12. Abaei, E., E. Mehrshai, and H. R. Sadreazami, “The influence of periodic discontinuities on propagation characteristics of substrate integrated waveguide,” *IEEE Asia-Pacific Conference on Applied Electromagnetics (APCAE)*, 2010.
 13. Itoh, T., *Numerical Techniques for Microwave and Millimeter-Wave Passive Structures*, John Wiley and Sons Pub., New York, 1989.
 14. Sharma, P. C. and K. C. Gupta, “Desegmentation method for analysis of two-dimensional microwave circuits,” *IEEE Trans. on Microw. Theory and Tech.*, Vol. 29, No. 10, 1094–1098, 1981
 15. Abaei, E. and E. Mehrshai, “Efficient desegmentation technique for analysis of planar circuits,” *6th German Microwave Conference*, 2011.
 16. Collin, R. E., *Field Theory of Guided Waves*, IEEE press, New York, 1991
 17. Elachi, C., “Waves in active and passive periodic structures: A review,” *IEEE Trans. on Microw. Theory and Tech.*, Vol. 64, No. 12, 1976.